

## Article

# New Antibacterial Secondary Metabolites from a Marine-Derived *Talaromyces* sp. Strain BTBU20213036

Fuhang Song<sup>1</sup> , Yifei Dong<sup>1</sup>, Shangzhu Wei<sup>2</sup>, Xinwan Zhang<sup>2</sup>, Kai Zhang<sup>1</sup> and Xiuli Xu<sup>2,\*</sup>

<sup>1</sup> School of Light Industry, Beijing Technology and Business University, Beijing 100048, China; songfuhang@btbu.edu.cn (F.S.); dongyifei1930201016@st.btbu.edu.cn (Y.D.); zhangkai2030302071@st.btbu.edu.cn (K.Z.)

<sup>2</sup> School of Ocean Sciences, China University of Geosciences, Beijing 100083, China; 2111180016@cugb.edu.cn (S.W.); zhangxinwan@cugb.edu.cn (X.Z.)

\* Correspondence: xuxl@cugb.edu.cn

**Abstract:** New polyketide-derived oligophenalenone dimers, bacillisporins K and L (**1** and **2**) and xanthoradone dimer rugulosin D (**3**), together with four known compounds, bacillisporin B (**4**), macrosporone D (**5**), rugulosin A and penicillide (**6** and **7**), were isolated from the marine-derived fungus *Talaromyces* sp. BTBU20213036. Their structures were determined by detailed analysis of HRESIMS, 1D and 2D NMR data, and the absolute configurations were determined on the basis of calculated and experimental electronic circular dichroism (ECD). The antibacterial and antifungal activities of these compounds were tested against Gram-positive—*Staphylococcus aureus*, Gram-negative—*Escherichia coli*, and fungal strain—*Candida albicans*. These compounds showed potential inhibitory effects against *S. aureus* with minimum inhibitory concentrations ranging from 0.195 to 100 µg/mL.

**Keywords:** marine-derived fungus; *Talaromyces* sp.; antibacterial; *Staphylococcus aureus*; polyketide



**Citation:** Song, F.; Dong, Y.; Wei, S.; Zhang, X.; Zhang, K.; Xu, X. New Antibacterial Secondary Metabolites from a Marine-Derived *Talaromyces* sp. Strain BTBU20213036. *Antibiotics* **2022**, *11*, 222. <https://doi.org/10.3390/antibiotics11020222>

Academic Editors: William N. Setzer and Jesus Simal-Gandara

Received: 14 January 2022

Accepted: 8 February 2022

Published: 10 February 2022

**Publisher's Note:** MDPI stays neutral with regard to jurisdictional claims in published maps and institutional affiliations.



**Copyright:** © 2022 by the authors. Licensee MDPI, Basel, Switzerland. This article is an open access article distributed under the terms and conditions of the Creative Commons Attribution (CC BY) license (<https://creativecommons.org/licenses/by/4.0/>).

## 1. Introduction

The discovery and introduction into clinics of antibiotics have made great contributions to human health. The most widely applied antibiotics in clinics were discovered in the period between the 1950s and 1960s, while the overuse of antibiotics lead to the emergence of drug-resistant bacteria, which is recognized globally by scientists nowadays [1,2]. The spread of multi-drug resistant microorganisms is getting more and more serious to humans [3–5]. It is estimated that 700,000 people died as a result of infections caused by antimicrobial resistant bacteria annually [6]. There is an urgent demand to screen new antibiotics in order to combat the infective diseases caused by drug-resistant bacteria.

Fungi from marine environments have proven to be important pools for structurally unique and biologically diverse natural products [7]. *Talaromyces* fungi belong to ascomycetous. A number of *Talaromyces* species have been isolated from marine environments, such as, *Talaromyces albiverticillius*, *Talaromyces assiutensis*, *Talaromyces purpureogenus* [8–12]. Fungi of *Talaromyces* genus isolated from marine environments produced a series of bioactive natural products, such as oligophenalenones [11–15], terpenoids [16,17], naphthoquinones [18], spolyene and isocoumarin [19], diphenyl ether derivatives, sesquiterpene-conjugated amino acids [20,21], lactones [22], and ergosterol analog and bisanthraquinone [23]. In the course of our continuing investigation of bioactive natural products from marine-derived fungi [24–26], the fungal strain *Talaromyces* sp. BTBU20213036, which was obtained from a mud sample collected from the coastal region of Qingdao, Shandong Province, exhibited antimicrobial activity against *Staphylococcus aureus*. Fermentation scale-up of this strain was conducted in rice solid media. The study of the chemical constituents of the fermentation materials resulted in the isolation and characterization of three new secondary metabolites, including bacillisporins K and L (**1** and **2**) and rugulosin D (**3**), together with

four known compounds, bacillisporin B [15], macrosporone D [27], rugulosin A [28] and penicillide [29] (Figure 1). 1, 2 and 4–6 showed potential antibacterial activities against *S. aureus*. Herein we report the details of isolation, structure elucidation, and antimicrobial activities evaluation of these compounds.

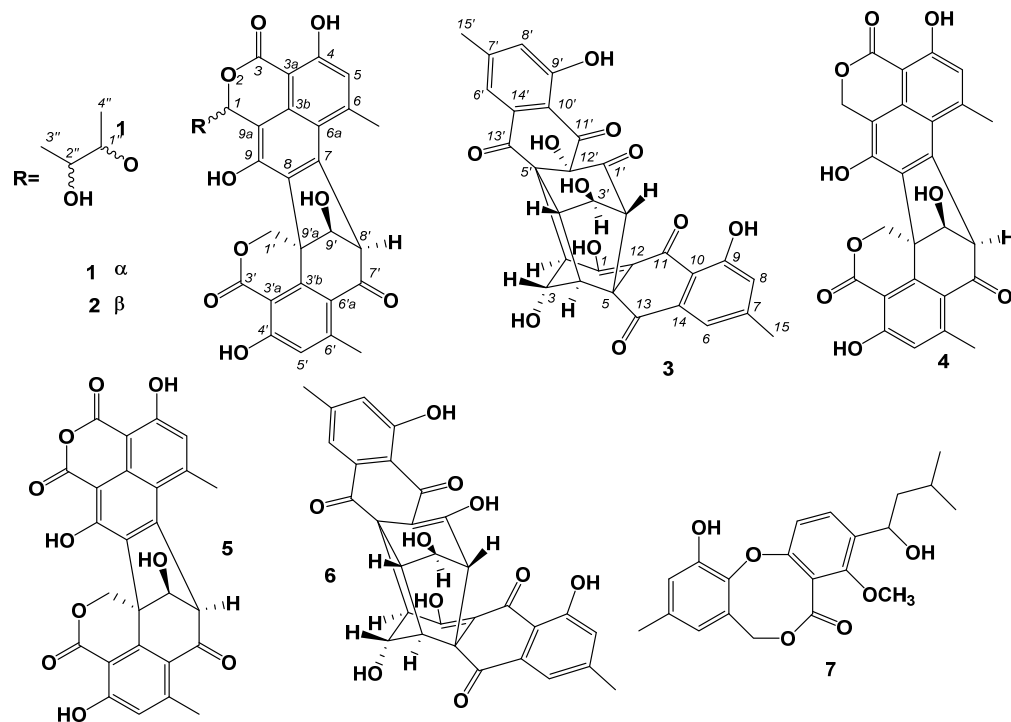


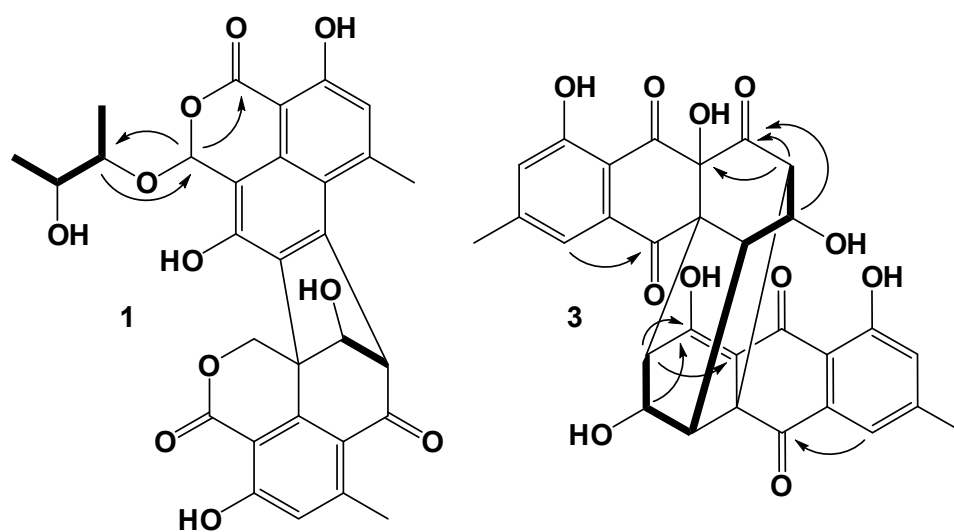
Figure 1. Chemical structures of 1–7.

## 2. Results

Compound 1 was isolated as a light yellow amorphous powder. The molecular formula of 1 was determined to be  $C_{30}H_{26}O_{11}$  based on high resolution electrospray ionization mass spectrum (HRESIMS) ( $m/z$   $[M + H]^+$  585.1374, calcd for  $C_{30}H_{27}O_{11}$ , 585.1367), accounting for eighteen degrees of unsaturation (Figure S1). Figure S2 showed the High Performance Liquid Chromatography (HPLC) profile and ultraviolet (UV) spectrum of 1. The  $^1H$ ,  $^{13}C$  and Heteronuclear Single Quantum Correlation (HSQC) spectra of 1 (Figures S3–S5, Table 1) showed the presence of four methyl groups [ $\delta_H$  2.98/ $\delta_C$  24.4 (6-Me),  $\delta_H$  2.48/ $\delta_C$  23.2 (6'-Me),  $\delta_H$  0.75/ $\delta_C$  15.6 (C-3''),  $\delta_H$  0.99/ $\delta_C$  17.2 (C-4'')], one oxygenated methylene group [ $\delta_H$  5.12 and 4.95/ $\delta_C$  69.9 (C-1')], five  $sp^3$  methine groups [ $\delta_H$  6.86/ $\delta_C$  98.8 (C-1),  $\delta_H$  4.83/ $\delta_C$  64.9 (C-8'),  $\delta_H$  4.77/ $\delta_C$  85.1 (C-9'),  $\delta_H$  4.12/ $\delta_C$  78.6 (C-1''),  $\delta_H$  3.72/ $\delta_C$  68.9 (C-2'')], two aromatic methines [ $\delta_H$  6.96/ $\delta_C$  118.4 (C-5),  $\delta_H$  6.83/ $\delta_C$  119.6 (C-5')], one  $sp^3$  quaternary carbon [ $\delta_C$  49.5 (C-9'a)], as well as seventeen  $sp^2$  quaternary carbons including one ketone carbonyl [ $\delta_C$  192.5 (C-7')] and two lactone carboxyls [ $\delta_C$  168.3 (C-3), 167.8 (C-3')].  $^1H$ - $^1H$  Correlation Spectroscopy (COSY) spectrum (Figure 2 and Figures S6) indicated the side chain of C-3''/C-2''/C-1''/C-4''. By comparing the NMR data with those of 5, one of the lactones was replaced by the acetal methine [ $\delta_H$  6.86 (s)/ $\delta_C$  98.8 (C-1)] and the linkage between C-1 and C-1'' through the oxygen atom was confirmed by Heteronuclear Multiple Bond Correlation (HMBC) correlations (Figure 2 and Figure S7, Table S1) from H-1 to C-3 and C-1'' and from H-1'' to C-1. The structure of 1 was further established by  $^1H$ - $^1H$  COSY (Figure 2 and Figure S6) and HMBC experiments. The relative configurations were deduced by the singlet peaks for H-8' [ $\delta_H$  4.83 (s)] and H-9' [ $\delta_H$  4.77 (brs)] and Rotating Frame Overhauser Spectroscopy (ROESY) correlation between H-8' and H-9' (Figure S8).

**Table 1.**  $^1\text{H}$  (500 MHz) and  $^{13}\text{C}$  NMR (125 MHz) data of **1**, **2** and **5** (in DMSO).

Position	1		2		5	
	$\delta_{\text{C}}$	$\delta_{\text{H}}$ (J in Hz)	$\delta_{\text{C}}$	$\delta_{\text{H}}$ (J in Hz)	$\delta_{\text{C}}$	$\delta_{\text{H}}$ (J in Hz)
1	98.8	6.86, s	99.5	6.81, s	165.1	
3	168.3		168.1		164.4	
3a	96.4		96.2		98.4	
3b	130.3		130.2		134.6	
4	162.5		162.4		162.5	
5	118.4	6.96, s	118.8	6.97, s	120.1	7.14, s
6	146.7		146.6		148.1	
6a	118.4		118.4		118.0	
7	139.6		139.8		149.0	
8	134.3		133.8		132.5	
9	152.2		152.4		160.8	
9a	109.0		109.4		100.3	
1'	69.9	5.12, d (12.0) 4.95, d (12.0)	69.7	5.12, d (12.0) 5.00, d (12.0)	69.4	5.18, d (12.5) 5.00, d (12.5)
3'	167.8		167.9		167.6	
3'a	103.7		103.7		104.0	
3'b	147.6		147.8		147.1	
4'	163.1		163.3		163.5	
5'	119.6	6.83, s	119.7	6.83, s	120.1	6.87, s
6'	152.2		152.4		152.5	
6'a	116.6		116.7		116.6	
7'	192.5		192.5		191.2	
8'	64.9	4.83, s	64.6	4.87, d (1.0)	65.5	4.99, s
9'	85.1	4.77, br s	85.6	4.78, d (5.0)	85.2	4.85, s
9'a	49.5		49.7		49.4	
Me-6	24.4	2.98, s	24.6	2.99, s	24.5	3.06, s
Me-6'	23.2	2.48, s	23.2	2.47, s	23.2	2.48, s
1''	78.6	4.12, m	80.2	3.90, m		
2''	68.9	3.72, m	71.3	3.61, m		
3''	15.6	0.75, d (6.5)	18.9	1.14, d (6.5)		
4''	17.2	0.99, d (6.5)	17.9	1.11, d (6.5)		
OH-9'		6.24, d (3.0)		6.31, d (3.0)		

**Figure 2.** Key  $^1\text{H}$ - $^1\text{H}$  COSY and HMBC correlations for **1** and **3**.

Compound **2** was isolated as a light yellow amorphous powder. The molecular formula of **2** was determined to be  $\text{C}_{30}\text{H}_{26}\text{O}_{11}$  based on the HRESIMS spectrum ( $m/z$   $[\text{M} + \text{H}]^+$  585.1377, calcd for  $\text{C}_{30}\text{H}_{27}\text{O}_{11}$ , 585.1367), accounting for eighteen degrees of

unsaturation (Figure S9). Figure S10 showed the HPLC profile and UV spectrum of **2**. The  $^1\text{H}$ ,  $^{13}\text{C}$  and HSQC spectra of **1** (Figures S11–S13, Table 1) showed similar data to those of **2**. The differences are signals for acetal methine [ $\delta_{\text{H}}$  6.81/ $\delta_{\text{C}}$  99.6 (C-1)] and the substructure attached to C-1 [ $\delta_{\text{H}}$  3.90/ $\delta_{\text{C}}$  80.2 (C-1''), 3.61/ $\delta_{\text{C}}$  71.3 (C-2''), 1.14/ $\delta_{\text{C}}$  18.9 (C-3''), 1.11/ $\delta_{\text{C}}$  17.9 (C-4'')]. These data revealed the configurations of C-1, C-1'', C-2'' were different from those of **2**, which resulted in the different deshielding effects from the aromatic moiety. Furthermore, the structure was characterized by detailed analysis of 2D NMR spectra (Figure 2 and Figures S13–S15). In the REOSY spectrum (Figure S16), the crossing peaks between H-8' and H-9'-OH, and between H-9' and H-1'a revealed the relative configurations of C-8', 9' and C-9a' (Table S2).

Compounds **1** and **2** showed almost the same experimental ECD spectra, which were consistent with the reported bacillisporin I [15] and calculated data (Figure 3). Thus, the configurations of **1** and **2** were determined as 8'R, 9'S, 9'aS, while the configurations of C-1, C-1'' and C-2'' were not determined. Compounds **1** and **2** were named bacillisporins K and L, respectively.

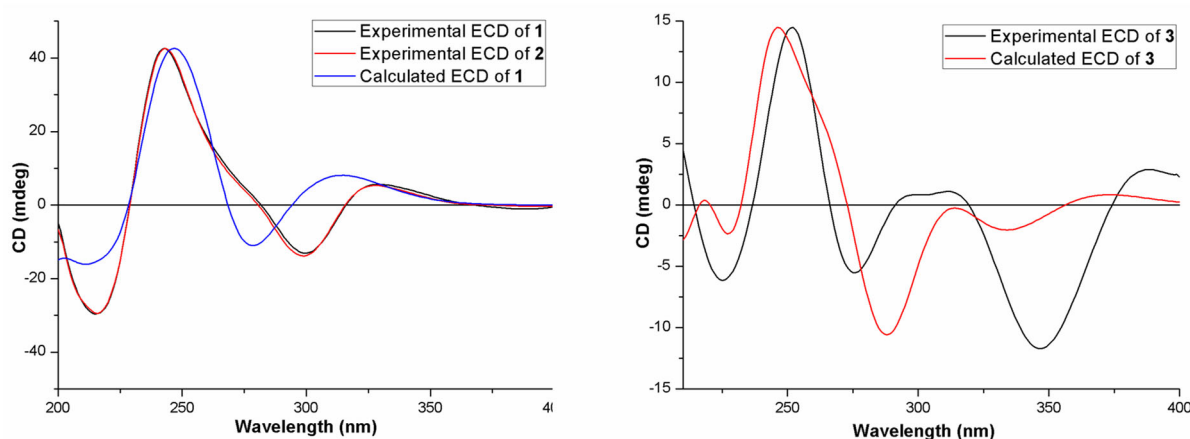


**Figure 3.** Experimental and calculated ECD spectra of **1**, **2** and **3**.

Compound **3** was isolated as a brown amorphous powder. The molecular formula of **3** was determined to be  $\text{C}_{30}\text{H}_{22}\text{O}_{11}$  based on the HRESIMS spectrum ( $m/z$  [ $\text{M} + \text{H}$ ] $^+$  559.1234, calcd for  $\text{C}_{30}\text{H}_{23}\text{O}_{11}$ , 559.1235), accounting for twenty degrees of unsaturation (Figure S17). Figure S18 showed the HPLC profile and UV spectrum of **3**. The  $^1\text{H}$ ,  $^{13}\text{C}$ , HSQC and  $^1\text{H}$ - $^1\text{H}$  COSY spectra of **2** (Figures S19–S22, Table 2) showed signals for two singlet methyl groups [ $\delta_{\text{H}}$  2.44/ $\delta_{\text{C}}$  21.6 (C-15),  $\delta_{\text{H}}$  2.43/ $\delta_{\text{C}}$  21.5 (C-15')], six  $\text{sp}^3$  methine groups [ $\delta_{\text{H}}$  2.73/ $\delta_{\text{C}}$  55.7 (C-2),  $\delta_{\text{H}}$  2.90/ $\delta_{\text{C}}$  63.4 (C-2'),  $\delta_{\text{H}}$  4.27/ $\delta_{\text{C}}$  70.2 (C-3),  $\delta_{\text{H}}$  4.56/ $\delta_{\text{C}}$  69.0 (C-3'),  $\delta_{\text{H}}$  3.46/ $\delta_{\text{C}}$  48.1 (C-4),  $\delta_{\text{H}}$  3.73/ $\delta_{\text{C}}$  44.0 (C-4')], four aromatic methines [ $\delta_{\text{H}}$  7.46/ $\delta_{\text{C}}$  120.6 (C-6),  $\delta_{\text{H}}$  7.41/ $\delta_{\text{C}}$  120.1 (C-6'), 7.24/ $\delta_{\text{C}}$  124.0 (C-8),  $\delta_{\text{H}}$  7.21/ $\delta_{\text{C}}$  123.8 (C-8')], three  $\text{sp}^3$  quaternary carbons including one oxygenated carbons [ $\delta_{\text{C}}$  74.6 (C-12')], five ketone carbonyls [ $\delta_{\text{C}}$  198.8 (C-1'), 184.8 (C-11),  $\delta_{\text{C}}$  192.1 (C-11'), 193.0 (C-13), 192.8 (C-13')], as well as ten  $\text{sp}^2$  quaternary carbons [ $\delta_{\text{C}}$  178.1 (C-1), 148.5 (C-7)/148.6 (C-7'), 160.9 (C-9)/161.0 (C-9'), 114.3 (C-10)/113.3 (C-10'), 106.8 (C-12), 132.3 (C-14)/133.5 (C-14')]. By comparing the NMR data with those of rugulosin A [28], the structure was deduced as an analogue of rugulosin A (**6**). Detailed analysis of the NMR data revealed that the  $\text{sp}^2$  quaternary carbons of C-1' [ $\delta_{\text{C}}$  186.7] and C-12' [ $\delta_{\text{C}}$  106.8] in rugulosin A were replaced by one ketone carbonyl [ $\delta_{\text{C}}$  198.8] and one oxygenated  $\text{sp}^3$  quaternary carbon [ $\delta_{\text{C}}$  74.6]. The planar structure of **3** further confirmed by HMBC correlations (Figure 2 and Figure S23, Table S3) from H-2' to C-1' and C-12'. The relative configurations of **3** were deduced by comparing the literature data for  $^1\text{H}$  NMR between rugulosin A and **3**, the chemical shifts of H-3/H-3' of **3** were  $\delta_{\text{H}}$  4.27/4.56 with a coupling constant of 5.0 and 4.5 Hz, which were almost the same as those reported for rugulosin A [28]. In the ROESY spectrum (Figure 4 and Figure S24), correlations between H-3' and H-2', H-4/H-4', and between H-3 and H-2 and H-4' were observed, which confirmed

the relative stereochemistry of **3**. By comparison of experimental and calculated ECD spectra (Figure 4), the absolute configurations of **3** were determined as shown in Figure 1 and named rugulosin D.

**Table 2.**  $^1\text{H}$  (500 MHz) and  $^{13}\text{C}$  NMR (125 MHz) NMR data of **3** and **6** (in DMSO).

Position	<b>3</b>		<b>6</b> [16]	
	$\delta_{\text{C}}$	$\delta_{\text{H}}$ (J in Hz)	$\delta_{\text{C}}$	$\delta_{\text{H}}$ (J in Hz)
1/1'	178.1/198.8		186.7	
2/2'	55.7/63.4	2.73, d (5.0)/2.90, d (4.5)	59.0	2.77, d (6.0)
3/3'	70.2/69.0	4.27, dd (5.0, 3.0)/4.56, dd (4.5, 4.0)	69.2	4.38, (dd, 6.0, 2.3)
4/4'	48.1/44.0	3.46, brs/3.73, brs	48.4	3.36, brs
5/5'	53.6/63.9		56.3	
6/6'	120.6/120.1	7.46, s/7.41, s	121.2	7.44, d (1.2)
7/7'	148.5/148.6		148.3	
8/8'	124.0/123.8	7.24, s/7.21, s	124.7	7.18, d (1.2)
9/9'	160.9/161.0		160.8	
10/10'	114.3/113.3		114.8	
11/11'	184.8/192.1		181.7	
12/12'	106.8/74.6		106.8	
13/13'	193.0/192.8		194.6	
14/14'	132.3/133.5		132.7	
15/15'	21.6/21.5	2.44, s/2.43, s	22.2	2.41, s
9-OH/	9-OH'	11.71, s/11.04, s		11.4, s

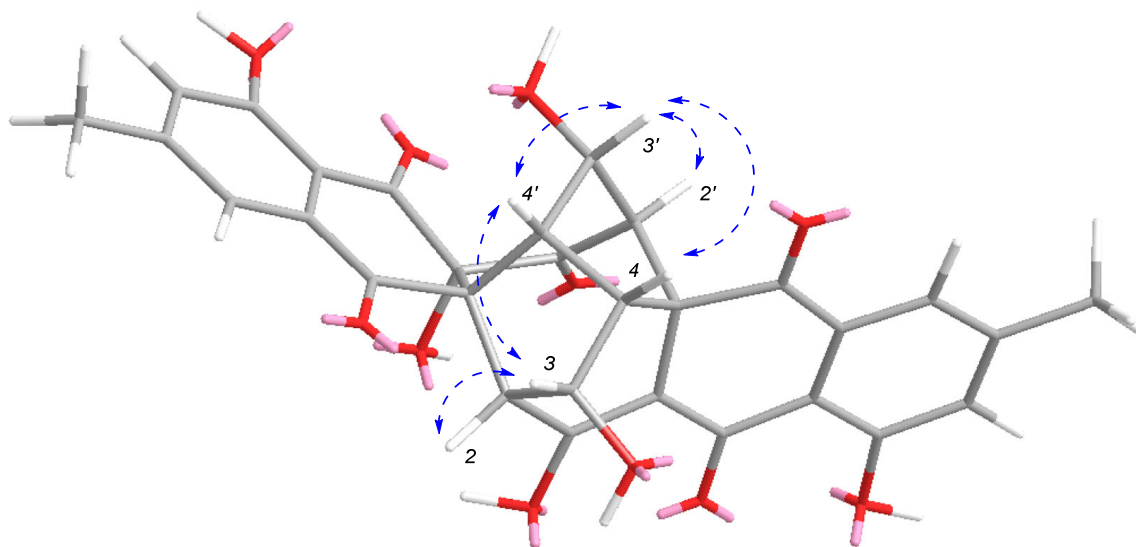


**Figure 4.** Key ROESY correlations of **3**.

Four known compounds, bacillisporin B [15], macrosporinone D [27], rugulosin A [28] and penicillide [29] were also isolated and characterized by comparing their molecular weight and NMR data with those reported in the literature.

These compounds were tested for antibacterial activities against a panel of pathogens of *S. aureus* ATCC 25923, *Escherichia coli* ATCC 25923 and *Candida albicans* ATCC 10231. Compounds **1**, **2** and **4–6** strongly inhibited the growth of *S. aureus* with MIC values of 12.5, 25, 12.5, 6.25, and 0.195  $\mu\text{g}/\text{mL}$  (Table 3). None of the tested compounds showed inhibitory effects against *C. albicans* and *E. coli* at concentration of 100  $\mu\text{g}/\text{mL}$ .

**Table 3.** Antibacterial activity of compounds 1–7 (MIC, µg/mL).

Number	1	2	3	4	5	6	7	Control
<i>C. albicans</i>	>100	>100	>100	>100	>100	>100	>100	1 <sup>a</sup>
<i>S. aureus</i>	12.5	25	>100	12.5	6.25	0.195	100	1 <sup>b</sup>
<i>E. coli</i>	>100	>100	>100	>100	>100	>100	>100	1 <sup>c</sup>

<sup>a</sup> Rapamycin, <sup>b</sup> Vancomycin, <sup>c</sup> Ciprofloxacin.

### 3. Materials and Methods

#### 3.1. General Experimental Procedures

Optical rotations ( $[\alpha]_D$ ) were measured by using an Anton Paar MCP 200 Modular Circular Polarimeter (Austria) in a 100 × 2 mm cell at 25 °C. CD spectra were recorded on Applied Photophysics Chirascan spectropolarimeter (Surrey, UK). NMR experiments were carried on a Bruker Avance 500 spectrometer at 25 °C with residual solvent peaks as references (DMSO-*d*<sub>6</sub>:  $\delta_H$  2.50,  $\delta_C$  39.52). High resolution ESIMS spectra were measured using an Accurate-Mass-Q-TOF LC/MS 6520 instrument (Santa Clara, CA, USA) in positive ion mode. HPLC was run on an Agilent 1200 Series instrument.

#### 3.2. Microbial Material

Strain BTBU20213036 was isolated from a mud sample collected from the intertidal zones of the Yellow Sea in Qingdao, China, and grown on a potato dextrose agar plate at 28 °C for 10 days. Colonies were about 25 mm diam, texture floccose and funiculate, sporulation abundant, dark greyish green, mycelium yellow, no exudate and soluble pigment, colony reverse brown (Figure S25). The genomic DNA of BTBU20213036 was extracted using DNAquick Plant System (Tiangen, Beijing, China). The ITS sequence of BTBU20213036 was amplified by using a conventional primer pair of ITS4 (5'-TCCTCCGCTTATTGATATGC-3') and ITS5 (5'-GGAAGTAAAAGTCGTAACAAGG-3'). PCR products were sequenced by Beijing Qingke Biotechnology Co., Ltd. (Beijing, China) and the sequence was deposited in GenBank (accession number, OM049426). Strain BTBU20213036 was identified as *Talaromyces* sp. based on gene sequence analysis of ITS by comparing with sequences from GenBank database using BLAST program (Figure S26). Alignments and calculations of sequence similarity were carried out using CLUSTAL W [30]. The strain was deposited in Beijing Technology and Business University, Beijing, China.

#### 3.3. Fermentation, Extraction and Purification

*Talaromyces* sp. BTBU20213036 was inoculated on a potato dextrose agar plate and incubated at 28 °C for 7 days. A slice of fungal colony of 1 cm<sup>2</sup> was put into twenty of 1 L conical flasks, each containing 200 g of raw rice, which was soaked in distilled water for 60 min. The inoculated flasks were incubated stationary at 28 °C for 30 days. The fermented materials of *Talaromyces* sp. BTBU20213036 were extracted three times by EtOAc:MeOH (80:20), and the organic solvent was evaporated in vacuo at 45 °C to yield brown crude extract (18.4 g). The crude extract was resuspended into 500 mL distilled water and extracted by 500 mL EtOAc (three times). Then EtOAc was evaporated *in vacuo* at 45 °C to give a dark residue (5.91 g). The EtOAc extract was separated by a reduced pressure silica gel chromatography (50 × 80 mm column, TLC H silica) with a stepwise gradient of 80–100% hexane/CH<sub>2</sub>Cl<sub>2</sub> and then 0–90% MeOH/CH<sub>2</sub>Cl<sub>2</sub> to afford 15 fractions. The eighth fraction was purified on a Sephadex LH-20 column using an elution of CH<sub>2</sub>Cl<sub>2</sub>:MeOH (2:1) to give four subfractions. The third subfraction was further separated by HPLC (Agilent ZORBAX SB-C18, 250 × 9.4 mm, 5 µm column, 3.0 mL/min) eluting with 40–50% MeCN/H<sub>2</sub>O in 15 min, then to 82% MeCN/H<sub>2</sub>O in 20 min to yield compounds 7 (10.2 mg), 5 (3.4 mg), 1 (4.9 mg), 4 (1.2 mg) and 2 (3.4 mg). The ninth fraction was subjected to a Sephadex LH-20 chromatography eluting by CH<sub>2</sub>Cl<sub>2</sub>:MeOH (2:1) to give four subfractions. The third subfraction was further purified by HPLC (Agilent ZORBAX Eclipse SB-C18, 250 × 9.4 mm, 5 µm column, 3.0 mL/min) eluting by 70% MeOH/H<sub>2</sub>O to give compounds

**3** (11.2 mg) and **6** (8.4 mg). The procedure for extraction and compounds isolation was shown in Figure S27.

### 3.3.1. Bacillisporin K (1)

Bacillisporin K (1): Light yellow amorphous powder;  $[\alpha]_D^{25} +206.0$  (c 0.1, MeOH);  $^1\text{H}$  and  $^{13}\text{C}$  NMR data, Table 1; HRESIMS  $m/z$  585.1374  $[\text{M} + \text{H}]^+$  (calcd for  $\text{C}_{30}\text{H}_{27}\text{O}_{11}$ , 585.1367).

### 3.3.2. Bacillisporin M (2)

Bacillisporin L (2): Light yellow amorphous powder;  $+231.5$  (c 0.2, MeOH);  $^1\text{H}$  and  $^{13}\text{C}$  NMR data, Table 1; HRESIMS  $m/z$  585.1377  $[\text{M} + \text{H}]^+$  (calcd for  $\text{C}_{30}\text{H}_{27}\text{O}_{11}$ , 585.1367).

### 3.3.3. Rugulosin D (3)

Rugulosin D (3): Brown amorphous powder;  $+18.0$  (c 0.2, MeOH);  $^1\text{H}$  and  $^{13}\text{C}$  NMR data, Table 2; HRESIMS  $m/z$  559.1234  $[\text{M} + \text{H}]^+$  (calcd for  $\text{C}_{30}\text{H}_{23}\text{O}_{11}$ , 559.1235).

## 3.4. Antibacterial Activity Assays

The antimicrobial activities were performed based on Antimicrobial Susceptibility Testing Standards outlined by the Clinical and Laboratory Standards Institute document M07-A7 (CLSI) [31] and our previous report [26] by using a panel of pathogens of *C. albicans* ATCC 10231, *S. aureus* ATCC 25923 and *E. coli* ATCC 25922. All the tested compounds were dissolved in dimethyl sulfoxide and diluted in two fold. The minimum inhibitory concentrations (MICs) were determined to be the lowest concentration with no visible bacterial in wells.

## 4. Conclusions

The chemical investigation of a marine-derived fungus *Talaromyces* sp. BTBU20213036 resulted in the isolation of three new compounds (**1–3**), and four previously reported metabolites (**4–7**). Among them, bacillisporins K and L shared dimeric oligophenalenone scaffold. Rugulosin D (**4**) is a dimer of the emodin-type anthraquinone. The absolute configurations of isolated compounds were determined by quantum chemical calculations of ECD. Compounds **1**, **2** and **4–7** displayed antibacterial activities against *S. aureus* with MIC values of 12.5, 25, 12.5, 6.25, 0.195 and 100  $\mu\text{g}/\text{mL}$ , respectively. The difference between **3** and **6** is that the hydroxymethine of C-12' in **3** was replaced by a  $\text{sp}^2$  quaternary carbon to form an  $\alpha,\beta$ -unsaturated ketene. The  $\alpha,\beta$ -unsaturated ketene moiety enhanced the antibacterial activity of **6** with 64 folds compared to that of **3**. The antibacterial activity of **6** (MIC = 0.195  $\mu\text{g}/\text{mL}$ ) is much stronger than the positive control of vancomycin (MIC = 1  $\mu\text{g}/\text{mL}$ ), which indicates it could be considered as a lead compound for further investigations into the mechanism and development of antibacterial agents.

**Supplementary Materials:** The following are available online at <https://www.mdpi.com/article/10.3390/antibiotics11020222/s1>, Figures S1–S24: HRESIMS, HPLC profiles, 1D and 2D NMR spectra for compounds **1–3**, Figures S25 and S26: Colony morphology and Neighbor-joining phylogenetic tree of strain BTBU20213036, Figure S27: Flow chart of the fermentation, extraction and isolation, Tables S1–S3: 1D and 2D NMR data for compounds **1–3**.

**Author Contributions:** Data curation, F.S., K.Z. and X.X.; Funding acquisition, F.S.; Investigation, F.S., Y.D., S.W., X.Z. and K.Z.; Supervision, X.X.; Writing—original draft, F.S. and X.X.; Writing—review and editing, F.S. and X.X. All authors have read and agreed to the published version of the manuscript.

**Funding:** This work was supported by grants from the National Natural Science Foundation of China (81973204), the Key Lab of Marine Bioactive Substance and Modern Analytical Technique, SOA (MBSMAT-2019-06), and Research Foundation for Advanced Talents of Beijing Technology and Business University (19008021176).

**Data Availability Statement:** Data are contained within the text.

**Conflicts of Interest:** The authors declare no conflict of interest.

## References

1. Shen, B. A new golden age of natural products drug discovery. *Cell* **2015**, *163*, 1297–1300. [[CrossRef](#)]
2. Jernigan, J.A.; Hatfield, K.M.; Wolford, H.; Nelson, R.E.; Olubajo, B.; Reddy, S.C.; McCarthy, N.; Paul, P.; McDonald, L.C.; Kallen, A.; et al. Multidrug-resistant bacterial infections in U.S. hospitalized patients, 2012–2017. *N. Engl. J. Med.* **2020**, *382*, 1309–1319. [[CrossRef](#)] [[PubMed](#)]
3. Arendrup, M.C.; Patterson, T.F. Multidrug-resistant *Candida*: Epidemiology, molecular mechanisms, and treatment. *J. Infect. Dis.* **2017**, *216*, S445–S451. [[CrossRef](#)] [[PubMed](#)]
4. Martínez-Vázquez, A.V.; Vázquez-Villanueva, J.; Leyva-Zapata, L.M.; Barrios-García, H.; Rivera, G.; Bocanegra-García, V. Multidrug resistance of *Escherichia coli* strains isolated from *Bovine Feces* and Carcasses in Northeast Mexico. *Front. Vet. Sci.* **2021**, *8*, 643802. [[CrossRef](#)] [[PubMed](#)]
5. Hiramatsu, K.; Katayama, Y.; Matsuo, M.; Sasaki, T.; Morimoto, Y.; Sekiguchi, A.; Baba, T. Multi-drug-resistant *Staphylococcus aureus* and future chemotherapy. *J. Infect. Chemother.* **2014**, *20*, 593–601. [[CrossRef](#)]
6. Ciloglu, F.U.; Caliskan, A.; Saridag, A.M.; Kilic, I.H.; Tokmakci, M.; Kahraman, M.; Aydin, O. Drug-resistant *Staphylococcus aureus* bacteria detection by combining surface-enhanced Raman spectroscopy (SERS) and deep learning techniques. *Sci. Rep.* **2021**, *11*, 18444. [[CrossRef](#)] [[PubMed](#)]
7. Carroll, A.R.; Copp, B.R.; Davis, R.A.; Keyzers, R.A.; Prinsep, M.R. Marine natural products. *Nat. Prod. Rep.* **2021**, *38*, 362–413. [[CrossRef](#)]
8. Venkatachalam, M.; Gérard, L.; Milhau, C.; Vinale, F.; Dufossé, L.; Fouillaud, M. Salinity and temperature influence growth and pigment production in the marine-derived fungal strain *Talaromyces albobiverticillius* 30548. *Microorganisms* **2019**, *7*, 10. [[CrossRef](#)]
9. Mishra, R.C.; Kalra, R.; Dilawari, R.; Deshmukh, S.K.; Barrow, J.; Goel, M. Characterization of an endophytic strain *Talaromyces assiutensis*, CPEF04 with evaluation of production medium for extracellular red pigments having antimicrobial and anticancer properties. *Front. Microbiol.* **2021**, *12*, 665702. [[CrossRef](#)]
10. Kumari, M.; Taritla, S.; Sharma, A.; Jayabaskaran, C. Antiproliferative and antioxidative bioactive compounds in extracts of marine-derived endophytic fungus *Talaromyces purpureogenus*. *Front Microbiol.* **2018**, *9*, 1777. [[CrossRef](#)]
11. Guo, Z.; Shao, C.; She, Z.; Cai, X.; Liu, F.; Vrijimoed, L.L.P.; Lin, Y. <sup>1</sup>H and <sup>13</sup>C NMR assignments for two oxaphenalenones bacillosporin C and D from the mangrove endophytic fungus SBE-14. *Magn. Reson. Chem.* **2007**, *45*, 439–441. [[CrossRef](#)] [[PubMed](#)]
12. Liang, X.; Huang, Z.H.; Shen, W.B.; Lu, X.H.; Zhang, X.X.; Ma, X.; Qi, S.H. Talaromyxaones A and B: Unusual oxaphenalenone spirolactones as phosphatase inhibitors from the marine-derived fungus *Talaromyces purpureogenus* SCSIO 41517. *J. Org. Chem.* **2021**, *86*, 12831–12839. [[CrossRef](#)] [[PubMed](#)]
13. Wu, B.; Ohlendorf, B.; Oesker, V.; Wiese, J.; Malien, S.; Schmaljohann, R.; Imhoff, J.F. Acetylcholinesterase inhibitors from a marine fungus *Talaromyces* sp strain LF458. *Mar. Biotechnol.* **2015**, *17*, 110–119. [[CrossRef](#)] [[PubMed](#)]
14. Wang, M.; Yang, L.; Feng, L.; Hu, F.; Zhang, F.; Ren, J.; Qiu, Y.; Wang, Z. Verruculosins A–B, new oligophenalenone dimers from the soft coral-derived fungus *Talaromyces verruculosus*. *Mar. Drugs* **2019**, *17*, 516. [[CrossRef](#)]
15. Dramaee, A.; Intaraudom, C.; Bunbamrung, N.; Saortep, W.; Srichomthong, K.; Pittayakhajonwut, P. Heptacyclic oligophenalenones from the soil fungus *Talaromyces bacillisporus* BCC17645. *Tetrahedron* **2020**, *76*, 130980. [[CrossRef](#)]
16. Huang, Z.H.; Liang, X.; Li, C.J.; Gu, Q.; Ma, X.; Qi, S.H. Talaromynoids A–I, highly oxygenated meroterpenoids from the marine-derived fungus *Talaromyces purpureogenus* SCSIO 41517 and their lipid accumulation inhibitory activities. *J. Nat. Prod.* **2021**, *84*, 2727–2737. [[CrossRef](#)]
17. Wang, W.; Wan, X.; Liu, J.; Wang, J.; Zhu, H.; Chen, C.; Zhang, Y. Two new terpenoids from *Talaromyces purpureogenus*. *Mar. Drugs* **2018**, *16*, 150. [[CrossRef](#)]
18. Liu, H.; Yan, C.; Li, C.; You, T.; She, Z. Naphthoquinone derivatives with anti-inflammatory activity from mangrove-derived endophytic fungus *Talaromyces* sp. SK-S009. *Molecules* **2020**, *25*, 576. [[CrossRef](#)]
19. Ma, M.Z.; Yi, W.W.; Qin, L.; Lian, X.Y.; Zhang, Z.Z. Talaromydien a and talaroisocoumarin A, new metabolites from the marine-sourced fungus *Talaromyces* sp. ZZ1616. *Nat. Prod. Res.* **2022**, *36*, 460–465. [[CrossRef](#)]
20. Nicoletti, R.; Trincone, A. Bioactive compounds produced by strains of *Penicillium* and *Talaromyces* of marine origin. *Mar. Drugs* **2016**, *14*, 37. [[CrossRef](#)]
21. Lan, D.; Wu, B. Chemistry and bioactivities of secondary metabolites from the genus *Talaromyces*. *Chem. Biodivers.* **2020**, *17*, e200022. [[CrossRef](#)]
22. Küppers, L.; Ebrahim, W.; El-Neketi, M.; Özkaya, F.C.; Mándi, A.; Kurtán, T.; Orfali, R.S.; Müller, W.E.G.; Hartmann, R.; Lin, W.; et al. Lactones from the sponge-derived fungus *Talaromyces rugulosus*. *Mar. Drugs* **2017**, *15*, 359. [[CrossRef](#)] [[PubMed](#)]
23. Noinart, J.; Buttachon, S.; Dethoup, T.; Gales, L.; Pereira, J.A.; Urbatzka, R.; Freitas, S.; Lee, M.; Silva, A.M.S.; Pinto, M.M.M.; et al. A new ergosterol analog, a new bis-antraquinone and anti-obesity activity of anthraquinones from the marine sponge-associated fungus *Talaromyces stipitatus* KUFA 0207. *Mar. Drugs* **2017**, *15*, 139. [[CrossRef](#)] [[PubMed](#)]
24. Song, F.; Lin, R.; Yang, N.; Jia, J.; Wei, S.; Han, J.; Li, J.; Bi, H.; Xu, X. Antibacterial secondary metabolites from marine-derived fungus *Aspergillus* sp. IMCASF180035. *Antibiotics* **2021**, *10*, 377. [[CrossRef](#)] [[PubMed](#)]
25. Xu, X.; Li, J.; Zhang, K.; Wei, S.; Lin, R.; Polyak, S.W.; Yang, N.; Song, F. New isocoumarin analogues from the marine-derived fungus *Paraphoma* sp. CUGBMF180003. *Mar. Drugs* **2021**, *19*, 313. [[CrossRef](#)]
26. Han, J.; Yang, N.; Wei, S.; Jia, J.; Lin, R.; Li, J.; Bi, H.; Song, F.; Xu, X. Dimeric hexylitaconic acids from the marine-derived fungus *Aspergillus welwitschiae* CUGBMF180262. *Nat. Prod. Res.* **2022**, *36*, 578–585. [[CrossRef](#)]

27. Chaiyosang, B.; Kanokmedhakul, K.; Sanmanoch, W.; Boonlue, S.; Hadsadee, S.; Jungsuttiwong, S.; Kanokmedhakul, S. Bioactive oxaphenalenone dimers from the fungus *Talaromyces macrosporus* KKU-1NK8. *Fitoterapia* **2019**, *134*, 429–434. [[CrossRef](#)]
28. Yamazaki, H.; Koyama, N.; Omura, S.; Tomoda, H. New rugulosins, anti-MRSA antibiotics, produced by *Penicillium radicum* FKI-3765-2. *Org. Lett.* **2010**, *12*, 1572–1575. [[CrossRef](#)]
29. Jeon, H.; Shim, S.H. Chemical constituents of the endophyte *Penicillium* sp. isolated from artemisia princeps. *Chem. Nat. Compd.* **2020**, *56*, 122–124. [[CrossRef](#)]
30. Thompson, J.D.; Higgins, D.G.; Gibson, T.J. Clustal-W—Improving the sensitivity of progressive multiple sequence alignment through sequence weighting, position-specific gap penalties and weight matrix choice. *Nucleic. Acids. Res.* **1994**, *22*, 4673–4680. [[CrossRef](#)]
31. Clinical and Laboratory Standards Institute. *Methods for Dilution Antimicrobial Susceptibility Tests for Bacteria that Grow Aerobically*, 7th ed.; Approved Standard; Clinical and Laboratory Standards Institute: Wayne, PA, USA, 2008.